INL/EXT-16-39882

# Radiation chemistry of the branched-chain monoamide di-ethylhexyl-isobutyramide

J. Drader, G. Saint-Louis, J. M. Muller,
M-C. Charbonnel, P. Guilbaud, L. Berthon,
K. Roscioli-Johnson, C. Zarzana,
G. Groenewold, B. J. Mincher,
S. P. Mezyk, K. McCann, J. Braley

September 2016


The INL is a U.S. Department of Energy National Laboratory
operated by Battelle Energy Alliance

INL/EXT-16-39882

# Radiation chemistry of the branched-chain monoamide di-ethylhexyl-isobutyramide

J. Drader, G. Saint-Louis, J. M. Muller, M-C. Charbonnel, P. Guilbaud, L. Berthon, K. Roscioli-Johnson, C. Zarzana, G. Groenewold, B. J. Mincher, S. P. Mezyk, K. McCann, J. Braley

September 2016

Idaho National Laboratory
Idaho Falls, Idaho 83415

http://www.inl.gov

Prepared for the
U.S. Department of Energy
Assistant Secretary for ____, OR Office of _____
Under DOE Idaho Operations Office
Contract DE-AC07-05ID14517

Report: FCRD-MRWFD-2016-000051
INL/EXT-16-39882

# Radiation chemistry of the branched-chain monoamide di-ethylhexyl-isobutyramide

J. Drader, G. Saint-Louis, J.M. Muller, M-C. Charbonnel, P. Guilbaud, L. Berthon
CEA Marcoule, Bagnols-sur-Cèze Cedex, F-30207, France

K. Roscioli-Johnson, C. Zarzana, G. Groenewold, B. J. Mincher
Idaho National Laboratory, Idaho Falls ID, 83415, USA

S.P. Mezyk
California State University, Long Beach, Long Beach, CA, 90840, USA

K. McCann, J. Braley
Colorado School of Mines, Golden, CO, 80401, USA

## INTRODUCTION

The dialkyl-monoamide class of extactant molecules has been studied for several decades as alternatives to tributylphosphate (TBP) in PUREX-type separations for the nuclear fuel cycle. Their advantages over TBP, as summarized in a review by Gasparini and Grossi,[1] include greater selectivity for uranium over fission products, higher radiolytic stability, generation of inoffensive radiolysis products, and the elimination of phosphorous. This latter point is referred to as adherence to the CHON principal in which reagents are composed of only carbon, hydrogen, oxygen and nitrogen, making them incinerable and thus preferable for waste treatment purposes.

An additional advantage of the dialkyl-monoamides over TBP is the ease of their synthetic tunability. This feature allows for metal ion selectivity to be designed into the structure of the monoamide. For example, although *n*-alkane substituted monoamides have overall higher extraction efficiencies for U(VI), branched-chain alkane-substituted monoamides are used for selection of U(VI) over Th(IV) and Pu(IV). Branching at the α-carbon of the alkane attached to the carbonyl carbon was shown to enhance extraction of uranium over the tetravalent ions including zirconium,[2] and to minimize third phase formation upon high metal loading.[3] Prabhu

et al. reported that *di*-2-ethylhexyl-butyramide (DEHBA) extracts U(VI) and Pu(IV), while *di*-2-ethylhexyl-*iso*butyramide (DEH*i*BA) selectively extracts U(VI), although with a lower $D_U$ than for the unbranched monoamide.[4] Thus, for applications involving U/Pu co-extraction, DEHBA would be preferred and for applications involving selective extraction of U, DEH*i*BA would be preferred. The structures of DEHBA and DEHiBA are shown in Fig. 1. In the Gasparini and Grossi review,[1] the stability of monoamides toward γ-radiolysis was reported to be relatively unaffected by the nature of the alkane groups, though Mowafy[5] reported that unsymmetrically substituted monoamides were more susceptible to radiolytic damage.

Although it has been commonly claimed that the monoamides have good radiation stability, there are few literature reports investigating this. They involve mainly post-irradiation studies of effects on solvent extraction and attempts to identify degradation products by spectroscopic or GC methods.[5–12] The major products are invariably reported to be the corresponding amine and organic acid, suggesting rupture of the carbonyl C-N bond. For example, Musikas[13,14] reported that the products of *di*-2-ethylhexyl-hexanamide radiolysis were *di*-2-ethylhexyl-amine and hexanoic acid. However, the secondary amine was produced in sub-stoichiometric amounts, suggesting that it hydrolyzed in the presence of acid. Similarly, Parikh et al.[8] identified the main products of *di*-hexyl-octanamide radiolysis using GC/GC-MS as *di*-hexyl-amine and octanoic acid. Uranium and plutonium extraction and subsequent stripping were unaffected by an absorbed dose of 600 kGy. This was attributed to the innocuous, water-soluble nature of the monoamide degradation products which is in stark contrast to the degradation products of tributylphosphate (TBP),[15] highlighting one of their advantages over the conventional extractant. Similarly, *di*-2-ethylhexyl-amine and *iso*butanoic acid were reported by Pathak et al. as the products of DEH*i*BA for irradiation in the presence of 3–4 M $HNO_3$, and the ability to strip the loaded solvent of uranium and plutonium was maintained even at 600 kGy absorbed dose.[9]

As the monoamides continue to be developed for potential application to the nuclear fuel cycle, research has been focused on the behavior of DEHBA and DEH*i*BA, ( Fig 1). The goal of this work is to provide a rigorous examination of the radiolytic decomposition of the uranium selective DEHiBA by identifying its degradation dose constants and products using mass spectrometry and measuring the impact on the extraction behavior of uranium(VI) by the irradiated solvent.

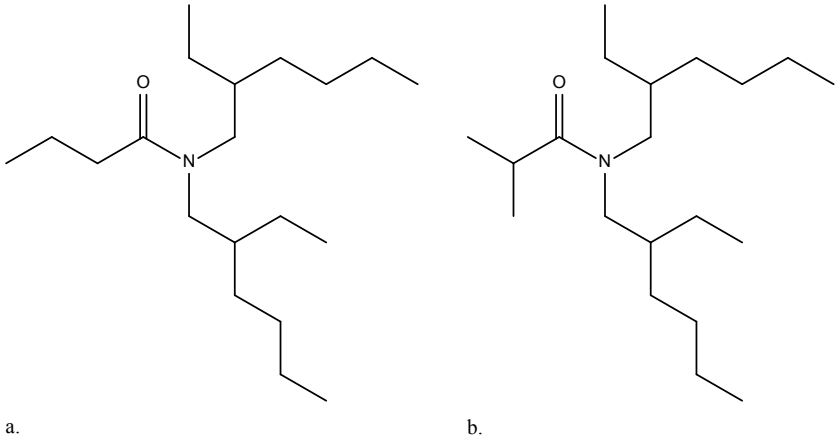


a. b.

**Figure 1.** Structure of *di-2-ethylhexyl-butyramide* (DEHBA), (a) and *di-2-ethylhexyl-isobutyramide* (DEH*i*BA), (b).

## EXPERIMENTAL

### Materials

The DEH*i*BA used in the preliminary work was prepared at Colorado School of Mines (USA) using a 1.2:1 molar ratio of *iso*-butyryl chloride diluted in chloroform, added dropwise to a mixture of the secondary amine, *bis*-2-ethylhexyl-amine, diluted in chloroform and *tri*-ethyl-amine. The dropwise addition was done in a nitrogen atmosphere at 5 °C under vigorous stirring. Once mixed, the solution was refluxed for 2 hours at 60 °C. This solution was then filtered and washed with water, 10 wt % sodium carbonate, and 1 M HCl to remove unreacted *tri*-ethyl-amine as well as residual *iso*-butyryl chloride. The solution was then dried with sodium sulfate

overnight. To purify the product, chloroform was removed by rotary evaporation followed by vacuum distillation. Characterization by $^{1}$H-NMR showed the product to be 99%+ pure. Upon the need for larger volumes for irradiations and solvent extraction, DEH*i*BA was purchased from Technocom (UK).

**Steady State Irradiations**

A 1 M solution of the monoamide was prepared by combining the appropriate amount of weighed DEH*i*BA in dodecane for irradiation. Samples were irradiated using a $^{60}$Co Nordion Gammacell 220, at a dose rate that varied from 4.73–4.34 kGy h$^{-1}$ during the course of the experiments. This dose rate was initially measured using standard Fricke procedures,[16] and then subsequently corrected for $^{60}$Co decay. The sample chamber temperature was approximately 30 $^{o}$C. The solutions were irradiated either as dry organic solutions, or in contact with either 0.1 M $HNO_3$ (stripping acidity), or 4 M $HNO_3$ (extraction acidity). In some cases, the samples were irradiated in static, sealed containers, considered deaerated upon exposure to even low absorbed doses. Some samples, as indicated in the text, were irradiated with air sparging at a rate of 1 mL min$^{-1}$, as delivered from a compressed air bottle through a mass flow controller. This was done to ensure that the samples so treated remained saturated with dissolved oxygen. Following irradiation, the samples were split for analysis by the collaborating laboratories at CEA-Marcoule and INL.

**Pulsed Irradiations**

Picosecond electron pulse radiolysis/transient absorption experiments were performed at the Brookhaven LEAF facility, as described previously.[17] Samples were irradiated in 1.00-cm Suprasil semimicro cuvettes sealed with Teflon stoppers. The doses per pulse for various experiments were in the range 20–40 Gy. Time-resolved kinetics were obtained using a FND-100

silicon diode detector and digitized using a LeCroy WaveRunner 640Zi oscilloscope (4 GHz, 8 bit). Interference filters (*10-nm bandpass) were used for the wavelength selection of the analyzing light.

**Analytical Measurements**

*ESI-MS analysis at CEA*

The mass spectrometry measurements were recorded in positive ion mode using a Bruker Esquire-LC quadrupole ion trap equipped with an electrospray interface. A Cole Palmer syringe infusion pump delivered the sample at a rate of 90 μL $h^{-1}$ to the electrospray source. The capillary voltage was set to –4000 V. Nitrogen was employed as the drying and nebulizing gas. The drying gas flow rate was 5.0 L $min^{-1}$ and the nebulizing gas pressure was set to 5.0 psi. The source temperature was 250 °C. Spectra were acquired over a mass/charge (m/z) range of 45–2200 with a trap drive setting of 50.0 at various skimmer voltages. Helium gas was used as the buffer gas in the trap to improve trapping efficiency and as a collision gas for fragmentation experiments.

Each sample was prepared by dilution in acetonitrile to a concentration of 1.0 x $10^{-4}$ M. To favor the ionization of compounds and avoid the formation of sodiated adducts, samples irradiated without an aqueous phase were acidified before analysis by addition of 1 drop of 1 M nitric acid. The ESI-MS measurements were taken within a short time after sample preparation to avoid any solvent influences on the speciation of degradation products. Species were identified by comparison with an isotopic pattern calculated using the software DataAnalysis 4.0. Ion trap CID was used to help identify the structure of various species through fragmentation studies.

*LC-ESI-MS analysis at INL*

Aliquots of the same samples were also analyzed at INL in positive ion mode, using a Dionex (Thermo Fisher, Sunnyvale, CA) UHPLC coupled to a Bruker (Billerica, MA) micro-TOFQ-II

electrospray ionization mass spectrometer. The mass spectrometer nitrogen drying gas flow rate was 9 mL $min^{-1}$, with a nebulizer gas pressure of 5.8 psi. The mass spectrometer conditions were a capillary voltage of –4000 V and a source temperature of 220 ºC. Samples were diluted by a factor of $10^3$ in 2-propanol followed by a factor of $4 \times 10^2$ in 50 % /50 % acetonitrile/water prior to analysis. The LC eluent was isocratic with 65% acetonitrile/35% 0.1% formic acid in water at a flow rate of 400 µL $min^{-1}$. Separations were achieved using 5 µL injections through a flow-through needle onto a Kinetex 1.3 µ C18 50 mm x 2.1 mm column (Phenomenex, Torrance, CA, USA). Each sample was analyzed in quintuplicate. DEHiBA was quantified using a calibration curve spanning the equivalent (accounting for dilution) of 2 M to 0.1 M DEHiBA. No standards were available for the degradation products, so their response is the integrated LC-MS peak area.

*FT-IR analysis at CEA*

Organic phase samples were analyzed with a Bruker vertex 70 spectrometer equipped with an attenuated total reflectance cell. All spectra were collected between 400–4000 $cm^{-1}$, using 32 scans and a resolution of 4 $cm^{-1}$.

**Uranium Solvent Extraction**

Uranium solvent extraction distribution ratios, $D_U$, were measured for both irradiated and non-irradiated solutions at INL. The aqueous phase contained 1 x $10^{-5}$ M natural uranium at the appropriate acidity. Preliminary experiments during this study showed that neither acid pre-equilibration of the organic phase, nor various contact times over the range of 30 sec–10 min affected the $D_U$ value. Subsequently the extractions reported here used non-pre-equilibrated, 30-sec, equal volume contacts at 23 ± 2 ºC. The maximum $D_U$ value was obtained at an initial aqueous phase acidity of 6.5 M $HNO_3$ and therefore all $D_U$ values were measured at this initial acidity. Stripping was performed using 0.1 M $HNO_3$ with 1-min contacts. The $D_U$ value was

determined as the ratio of the concentrations of uranium measured in the two phases after the contact. These concentrations were determined by mass spectrometry using a Thermo X series 2 ICP-MS with a Teflon sample introduction system and platinum cones. During analysis of organic solutions, 0.2 L $min^{-1}$ of 20 % oxygen in argon was added to the spray chamber to aid in combustion of the organic material and to reduce build up on the cones. Organic solutions were emulsified with Triton TX100 into the normal 1 % nitric acid solution used to dilute samples prior to analysis. Mass balances were calculated by comparison to the initial aqueous feed uranium concentration and averaged 98 ± 6 %.

## RESULTS AND DISCUSSION

### Degradation rates for monoamide radiolysis

By monitoring the concentration of the monoamide in organic solution as a function of absorbed dose, the concentration-dependent rate of degradation ($G$, μmol $J^{-1}$) and the concentration-independent dose constant ($d$, $kGy^{-1}$) can be determined. It was found that the concentration of DEH*i*BA decreased as absorbed dose increased, as shown in Fig 2. The rate was slow and approximately 70% of the initial monoamide concentration remained intact even at an absorbed dose of 1000 kGy, under all conditions of acidity and aeration. Given the small change in concentration, the data in these plots are modeled equally well using exponential or linear fits.

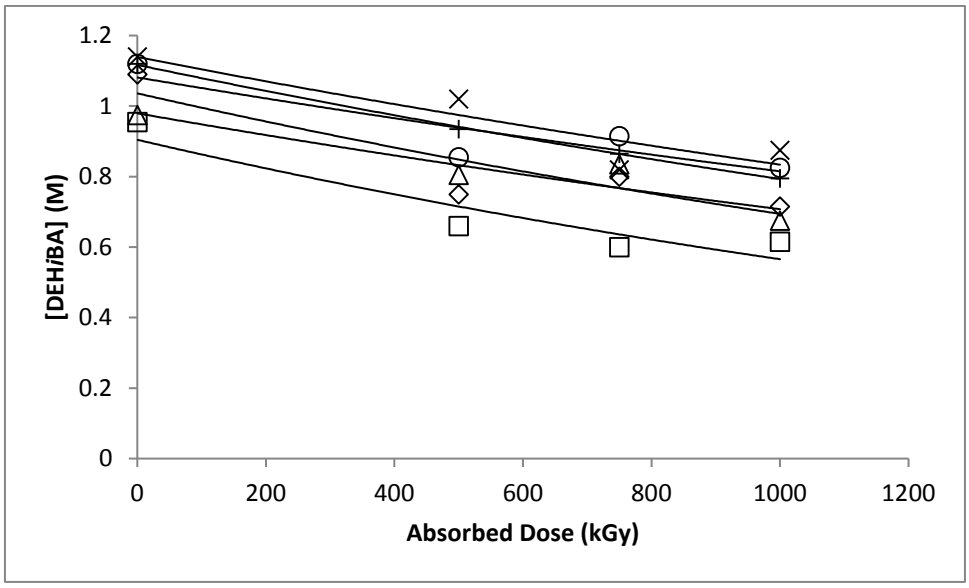


**Figure 2**. Change in DEH*i*BA concentration as a function of absorbed dose, for the organic phase only (+); organic phase with air sparging (circles); in contact with 0.1 M $HNO_3$ (diamonds); 0.1 M $HNO_3$ with air sparging (squares); 4 M $HNO_3$ (triangles); and 4 M $HNO_3$ with air sparging (×). Each datum is the mean of five injections with an average CI = 5.6%.

Exponential curve fitting was used to determine the dose constants (*d*) for monoamide degradation as the exponential constants of each equation. These values ranged from 2.8 x $10^{-4}$ $kGy^{-1}$ for the aerated organic sample to 4.7 x $10^{-4}$ $kGy^{-1}$ for the 0.1 M $HNO_3$-contacted organic phase, aerated sample for the curves shown in Figure 2. When the complete irradiation and analyses were repeated for samples prepared from a completely separate source of DEH*i*BA, *d* ranged from 2.5 x $10^{-4}$ $kGy^{-1}$ for the deaerated organic to 4.9 x $10^{-4}$ $kGy^{-1}$ for the aerated organic. These values, along with the $R^2$ values for the exponential fits to the data, are shown in Table 1.

As can be seen in Table 1, no trends in *d* are found with regard to the aqueous phase or aeration condition. This suggests that all conditions had roughly the same degradation kinetics, and the range is attributable to the difficulties inherent in measuring the small concentration change that occurred across these absorbed doses. The mean value for all conditions for both trials in Table 1 is (3.5 ± 0.78) x $10^{-4}$ $kGy^{-1}$. If the value with the very poor $R^2$ of 0.37 is

discounted, the mean becomes (3.6 ± 0.75) x $10^{-4}$ $kGy^{-1}$. It is concluded that the rate constant for DEH*i*BA radiolytic degradation is essentially identical across all conditions of acidity and aeration investigated here.

These results are similar to those previously reported for diglycolamides,[17,18,19] where the aqueous phase and aeration had little or no effect on degradation rates. However, the rate of monoamide degradation is about a factor of 10 slower than for the diglycolamides.[17,18] The stability measured here seems to be of the same order of magnitude as that found for malonamides irradiated after contact with an aqueous phase of water or 1–4 M nitric acid.[20] In that study, approximately 70-80 % of the initial concentration of three different malonamides remained after an absorbed dose of 750 kGy.

In spite of the large body of literature examining TBP radiolysis, few *G*-values have been reported for irradiation under conditions of contact with the acidic aqueous phase, and typically the yield of the main decomposition product dibutylphosphoric acid (HDBP) is reported instead of the actual decrease in TBP concentration. These $G_{HDBP}$ fall in the range of 0.05–0.5 μmol $J^{-1}$ for alkane solutions in the absence of the aqueous phase,[15] but obviously underestimate the actual $-G_{TBP}$. Adamov reported $-G_{TBP}$ = 0.37 μmol $J^{-1}$ in the presence of acid.[21] If the mean dose constant reported here of 3.5 x $10^{-4}$ $kGy^{-1}$ is used to calculate a *G*-value[17] for the loss in initially 1 M DEH*i*BA, the resulting $-G_{DEHiBA}$ = 0.45 μmol $J^{-1}$, comparable to TBP.

**Table 1**. Dose constants (*d*, $kGy^{-1}$) for the degradation of DEH*i*BA (trial 1 fits to data of Fig 2; trial 2 -separate data) under various conditions of irradiation.

| Condition | DEH*i*BA trial 1 | $R^2$ | DEH*i*BA trial 2 | $R^2$ |
|---|---|---|---|---|
| Organic deaerated | 3.4 x $10^{-4}$ | 0.99 | 2.5 x $10^{-4}$ | 0.37 |
| Organic aerated | 2.8 x $10^{-4}$ | 0.78 | 4.9 x $10^{-4}$ | 0.97 |
| 4 M $HNO_3$ deaerated | 3.3 x $10^{-4}$ | 0.85 | 4.2 x $10^{-4}$ | 0.92 |

| | | | | |
|---|---|---|---|---|
| 4 M $HNO_3$ aerated | 3.1 x $10^{-4}$ | 0.80 | 3.2 x $10^{-4}$ | 0.98 |
| 0.1 M $HNO_3$ deaerated | 4.0 x $10^{-4}$ | 0.81 | 2.9 x $10^{-4}$ | 0.84 |
| 0.1 M $HNO_3$ aerated | 4.7 x $10^{-4}$ | 0.86 | 2.8 x $10^{-4}$ | 0.96 |

Mean of all values = (3.5 ± 0.78) x $10^{-4}$ $kGy^{-1}$

**Organic phase analysis-FTIR**

To gain information about the nature of the degradation products formed under different experimental conditions, IR analysis was performed. Figures 3 and 4 show a comparison of the sample spectrum before irradiation and after, for two conditions: irradiation with no aqueous phase present and irradiation with 4 M $HNO_3$ present, respectively. Figure 3 compares the impact of irradiation alone to air sparging during irradiation on monoamide degradation without an aqueous phase present. The solid line represents 1 M DEH*i*BA dissolved in dodecane before irradiation. Upon irradiation, there appears to be little impact on the nature of the degradation products in the non-air sparged sample. This could indicate that the degradation products generated by irradiation maintain similar functional groups as the parent monoamide and are thus not unambiguously observable by IR.

In the air sparged sample, the spectra are slightly different. A shoulder appears at 1175 $cm^{-1}$ which could represent a C-N stretch in an aliphatic amine. A new peak is also observed at 1730 $cm^{-1}$ and as well as a shoulder peak at 1625 $cm^{-1}$. The appearance of the peak at 1730 $cm^{-1}$ might indicate formation of a new amide or a carboxylic acid (both common degradation products previously reported for monoamides). Development of the shoulder peak at 1625 $cm^{-1}$ could further indicate formation of a new amide species by representing a shift in amide functionality. Other species that are commonly generated during monoamide degradation that would show C=O

stretches in this region include ketones and esters. Interestingly, based on this comparison, air-sparging of the sample during irradiation changes the nature of the degradation products formed compared to irradiation under anaerobic conditions.

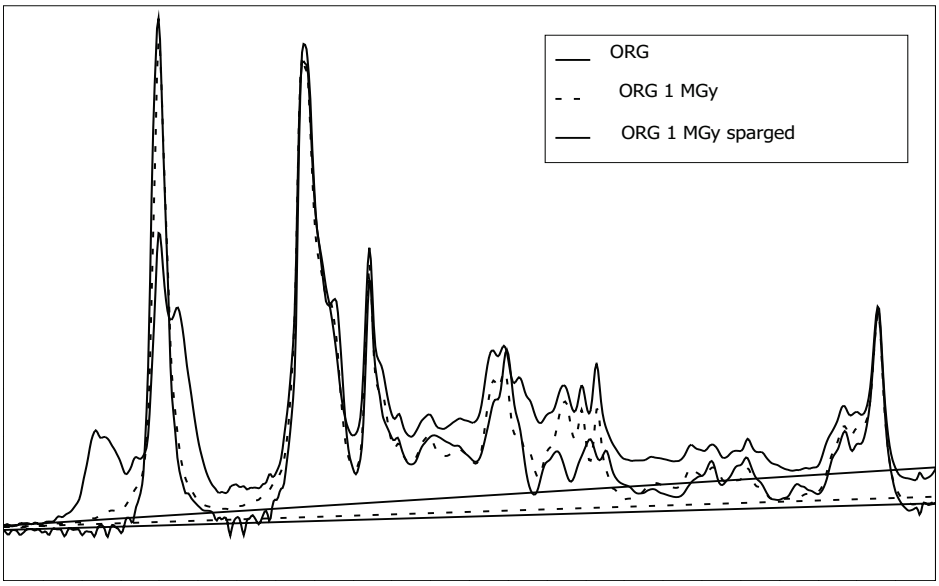


**Figure 3**. FTIR spectra of 1 M DEH*i*BA dissolved in dodecane (solid black line), 1 M DEH*i*BA dissolved in dodecane irradiated to 1 MGy (dashed line), 1 M DEH*i*BA dissolved in dodecane irradiated to 1 MGy with air sparge (dotted line).

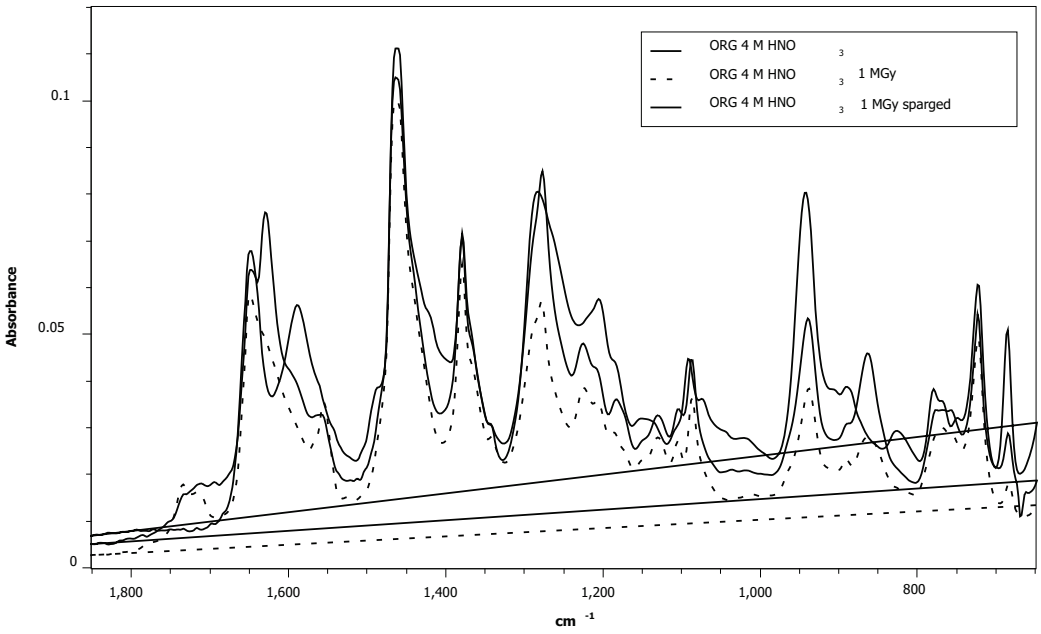

**Figure 4**. FTIR spectra of 1 M DEH*i*BA dissolved in dodecane contacted with 4 M $HNO_3$ (solid black line), 1 M DEH*i*BA dissolved in dodecane irradiated to 1 MGy while in contact with 4 M $HNO_3$ (dashed line), 1 M DEH*i*BA dissolved in dodecane irradiated to 1 MGy and air sparged while in contact with 4 M $HNO_3$ (dotted line).

When the sample is irradiated in the presence of acid, slightly different spectra are observed, (Fig. 4). The solid line in Fig. 4 represents 1 M DEH*i*BA dissolved in dodecane contacted with 4 M $HNO_3$. The spectrum of this sample shows a new $HNO_3$-monoamide peak at 1587 $cm^{-1}$ which has been assigned as the C=O group bonded to $HNO_3$.[19,22,23] Other new bands appear at 1284 $cm^{-1}$, 940 $cm^{-1}$, 827 $cm^{-1}$, and 686 $cm^{-1}$, all of which are consistent with the presence of nitric acid in the organic phase. After irradiation, in the both the air sparged and non-air sparged samples, the same peaks appear as were observed in the air sparged sample of the organic-only irradiated sample: 1730 $cm^{-1}$ and 1625 $cm^{-1}$. These likely represent bands from the same or similar degradation products that were observed in the aerated, organic-only sample. Interestingly, there is a clear decrease in the absorbance of the bands representing the C=O-$HNO_3$ stretch (1587 $cm^{-1}$ and 827 $cm^{-1}$) upon irradiation for both the air sparged and non-air sparged samples. This is consistent with a decrease of the nitric acid concentration in the organic phase after irradiation.

The conclusions from this analysis are that under both oxidizing conditions of acid and air sparging, similar degradation products are formed and these are slightly different than those that form due to irradiation of the deaerated organic phase alone. To identify these products, the samples were analyzed by mass spectrometry.

**Organic phase analysis-ESI-MS**

Mass spectra of the irradiated and non-irradiated samples show both the protonated and sodiated parent monomer and dimer compounds at m/z = 312.2, 334.2 and m/z = 623.0, 645.5,

respectively. Also observed in the spectra of irradiated and non-irradiated samples is a product at m/z 242.2 corresponding to *bis*-2-ethylhexyl-amine (DEHA), produced by carboxyl C–N bond rupture. It should be noted that though traces of DEHA were also found in non-irradiated samples, likely as an impurity from synthesis, it was also clearly generated during irradiation. Table 2 includes a summary of all degradation products found with an indication of specific experimental conditions under which they were formed. Most products were detected regardless of the experimental conditions though the relative yields of the degradation products were affected by the experimental conditions.

In the low molecular weight region of the mass spectra of the irradiated solutions, several degradation products were detected (see Table 2). The ESI-MS spectra for two of the aqueous phase conditions (no aqueous phase, 4 M $HNO_3$) are shown in Fig. 5. These conditions were shown since the spectra of the 0.1 M $HNO_3$ samples gave only intermediate results between these conditions and did not provide any additional insight.

In addition to the sub-monoamide mass region, a new peak is observed at m/z 310.2 as well as at values slightly higher than the m/z 312.2 of the monoamide. The product observed at m/z 310.2 corresponds to the abstraction of 2 hydrogen atoms from the ligand to form a C=C bond within the monoamide framework. This product was observed regardless of acid concentration and air sparging conditions. For samples in contact with the aqueous phase the most likely reactive species to react by H-atom abstraction is the $^{\bullet}OH$ radical, which reacts with alkanes with fast rate constants. The same product was found under aqueous-free conditions. In this case, the monoamide may react with dodecane radical cations by electron transfer. This has been reported previously for the diglycolamides.[17] If so, the loss of H-atoms may occur through proton elimination by the resulting monoamide radical cation (Eq. 1).

Addition of an •OH radical to the m/z 310.2 ion would generate the ion seen at m/z 328.0. However, this product was also observed in organic-only solution and another oxidative mechanism may account for its appearance. The product at m/z 258.2 could be produced either by carbonyl C–N bond rupture of the parent monoamide, or by H-atom abstraction from the amine N–H bond of DEHA, followed by addition of OH to generate *di*-2-ethylhexyl-hydroxyamine. This probably results from simple •OH radical addition to the produced •N radical. This product was observed only in air-sparged solutions at both acid concentrations. The product at m/z 200.2 corresponds to a C–N bond rupture resulting in the loss of one of the 2-ethylhexyl groups to produce *mono*-2-ethylhexyl-*iso*butyramide (EH*i*BA). This species was detected more at lower absorbed doses in the organic-only samples than in the 4 M $HNO_3$ contacted samples, perhaps suggesting that it is susceptible to acid hydrolysis.

**Table 2**. Compounds observed in the organic phase as a function of experimental conditions. L stands for DEH*i*BA. N.S. stands for Non Sparged samples and S for sparged samples

| m/z | Formula | Unirrad. | Org. only | | 0.1 M $HNO_3$ | | 4 M $HNO_3$ | |
|---|---|---|---|---|---|---|---|---|
| | | | N. S. | S. | N. S. | S. | N. S. | S. |
| 198 | $[C_{12}H_{22}NO]H^+$ | | | | | | X | |
| 200.2 | $[C_{12}H_{24}NO]H^+$ | | X | X | X | X | X | X |
| 236.1 | | | | | | X | | |
| 240.2 | $[C_{16}H_{33}N]H^+$ | | X | | X | | X | X |
| 242.2 | $[C_{16}H_{35}N]\ H^+$ | X | X | X | X | X | X | X |
| 254.1 | $[C_{16}H_{31}NO]H^+$ | | | | X | | X | X |
| 256.0 | $[C_{16}H_{33}NO]H^+$ | | X | X | | X | | |
| 258.2 | $[C_{16}H_{35}NO]H^+$ | | | | | X | | X |
| 270.3 | | | | X | | | | |
| 284.3 | | | | | X | | | |
| 292.1 | | | | | | X | | X |
| 296.2 | | | | | X | | | |
| 298.3 | | | | | X | | | |
| 310.2 | $[C_{20}H_{39}NO]H^+$ | | X | X | X | X | X | X |
| 312.2 | LH+ | X | X | X | X | X | X | X |
| 326.0 | $[C_{20}H_{39}NOO]H^+$ | | X | X | X | X | | X |
| 328.0 | $[C_{20}H_{40}NOOH]H^+$ | | X | X | X | X | X | |
| 334.2 | $LNa^+$ | X | X | X | X | X | X | |
| 340.2 | $[C_{20}H_{37}NO_3]H^+$ | | X | | X | | | |
| 348.2 | | | | | | X | | |
| 350.0 | $LK^+$ | X | X | X | X | X | X | X |
| 354.0 | | X | X | | | | | |
| 364.2 | | | | | | X | | |
| 379.2 | | | | | | | X | |
| 380.1 | | | | | | X | | |
| 395.3 | | | | | | | | X |
| 408.4 | $[C_{28}H_{57}N]H^+$ | | X | | X | | | |
| 410.5 | $[C_{28}H_{59}N]H^+$ | | X | | X | | | |
| 480.5 | $[C_{32}H_{65}NO]H^+$ | | X | X | X | | | |
| 533.5 | | | X | | X | X | | |
| 549.5 | $[C_{36}H_{72}N_2O]H^+$ | | X | | X | X | | |
| 551.7 | $[C_{36}H_{74}N_2O]H^+$ | | X | | X | | | |
| 603.3 | | | | | | X | | X |
| 623.0 | $L_2H^+$ | X | X | X | | X | X | X |
| 645.5 | $L_2Na^+$ | X | X | X | X | X | X | X |
| 661.1 | $L_2K^+$ | X | | | X | X | X | X |

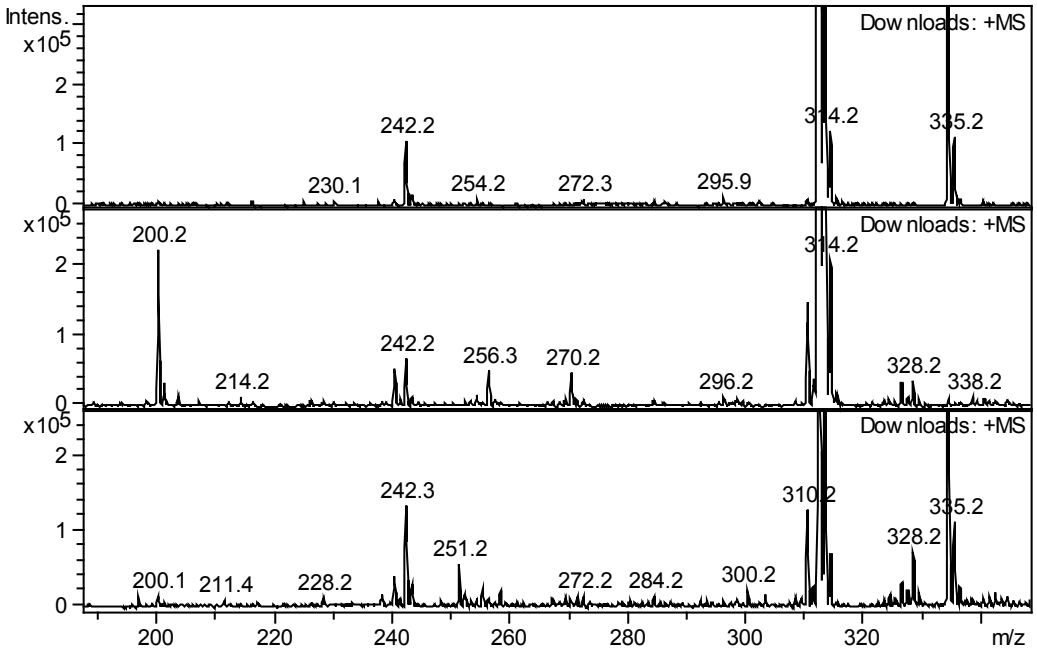


**Figure 5**. ESI-MS spectra of DEH*i*BA at 0 kGy (top), 1000 kGy organic phase only (middle), 1000 kGy contacted with 4 M $HNO_3$ (bottom). All spectra were recorded in positive ionization mode, trap drive 50, skimmer voltage 30 V, non-air sparged.

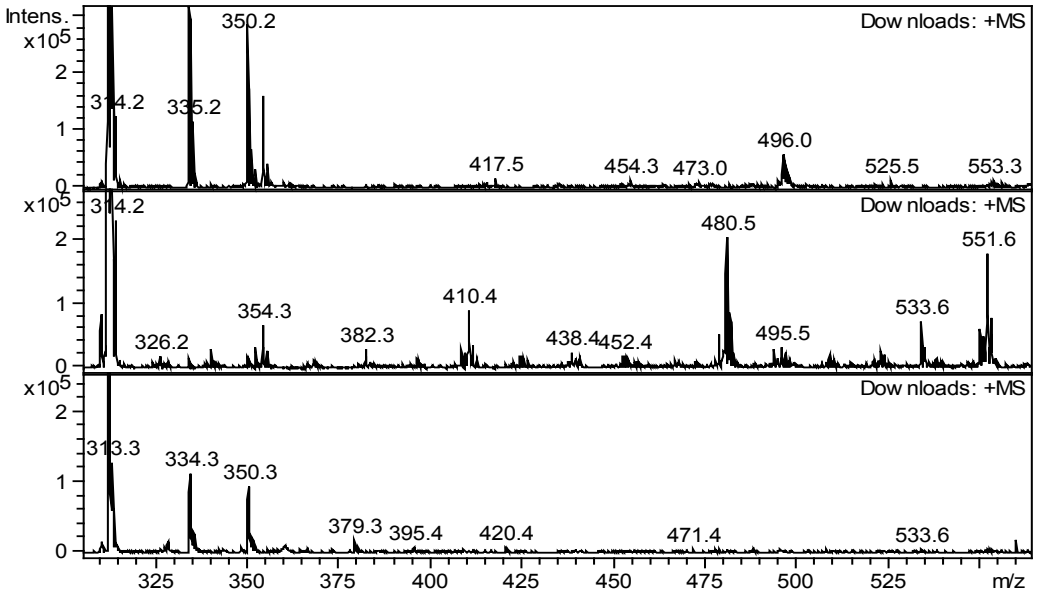


**Figure 6**. ESI-MS spectra of DEH*i*BA at 0 kGy (top), 750 kGy organic phase only (middle), 750 kGy contacted with 4 M $HNO_3$ (bottom). All spectra were recorded in positive ionization mode, trap drive 50, skimmer voltage 30 V, non-air sparged.

For products of higher molecular weight, (Fig. 6), new species appeared at m/z 551.7, 533.5, 480.5, and 410.5. Spectra generated by $MS^2$ fragmentation suggest that m/z 551.7 is an addition product of the monoamide with the amine DEHA. Two addition species between the dodecane or degradation products were identified at m/z 480.5 (monoamide + dodecane) and 410.5 (DEHA + dodecane). These high molecular weight species are likely produced by the addition reactions of the carbon-centered radicals generated by H-atom abstractions from the corresponding reactants. The peak at m/z 533.5 is unidentified.

Interestingly, the higher molecular weight products were observed to have the highest intensity in the samples not contacted with an aqueous phase during irradiation (Fig. 6). For samples irradiated in the presence of 0.1 M $HNO_3$, the abundance of these species was less intense. In the spectra of the samples irradiated in the presence of 4 M $HNO_3$ these species are completely absent. This could indicate that the C-centered radicals were scavenged by produced $^{\bullet}NO_3$ radicals under those conditions, although it must be noted that no nitro-substituted species were detected. Many of these nitro-, or hydroxy-substituted species may have reported to the aqueous phase.

It is clear that the presence of acid during irradiation of the monoamide ligand impacts the formation of higher molecular weight species. Thus, there appear to be competitive degradation pathways for DEH*i*BA degradation; an acid promoted pathway; Scheme 1, and an acid independent pathway; Scheme 2.

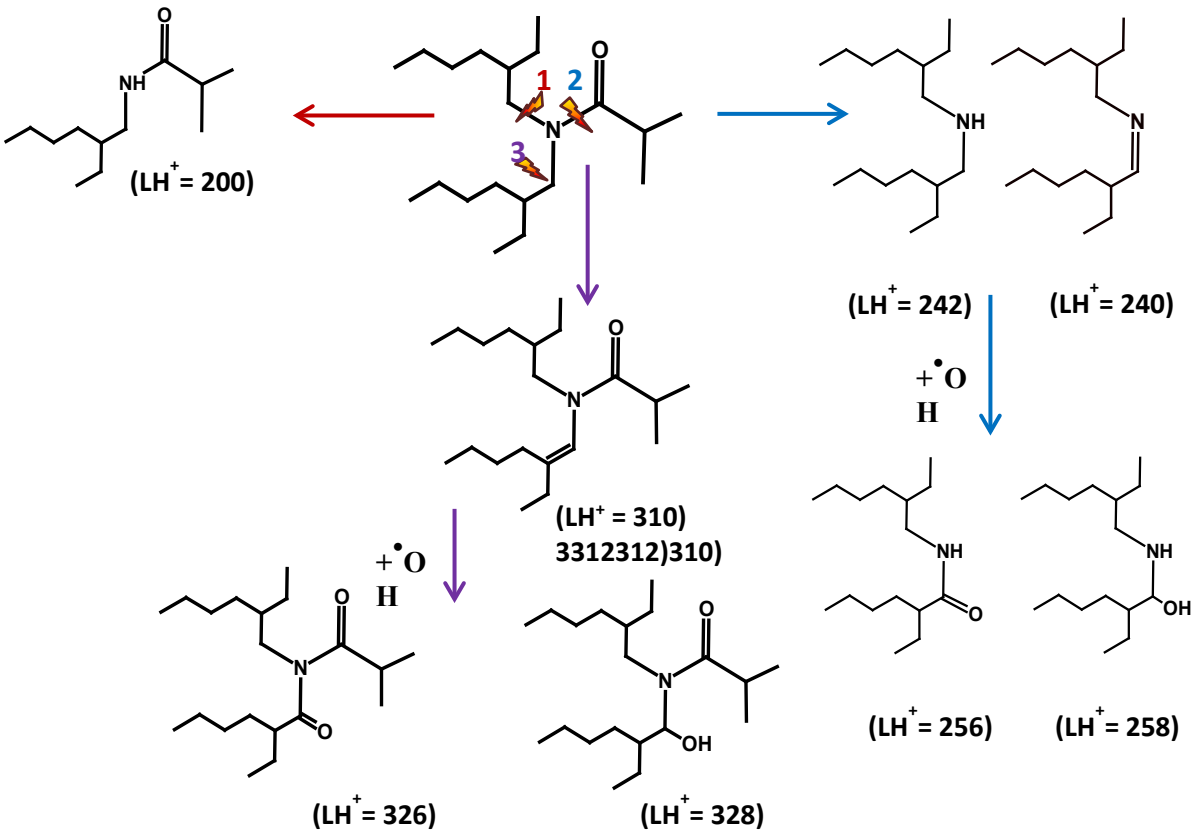


**Scheme 1**. Proposed DEH*i*BA degradation pathway in the presence of acid.

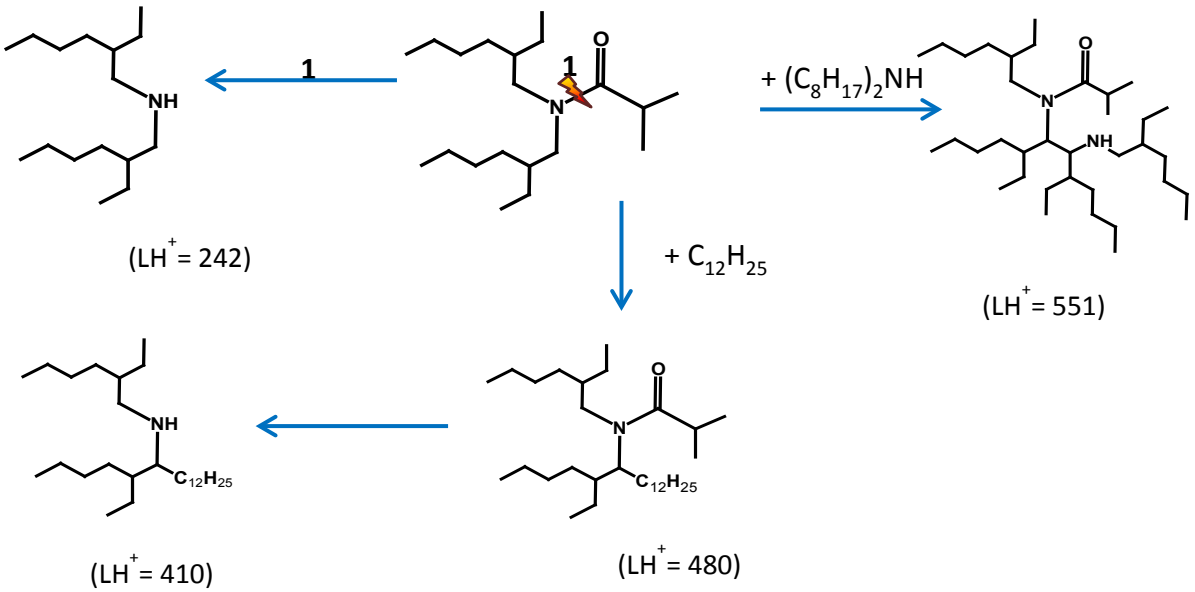


**Scheme 2**. Proposed DEH*i*BA degradation pathway in the absence of acid.

This conclusion correlates well with the FTIR data collected by supporting the observation that the samples irradiated in the presence of acid resulted in new peaks in the spectrum, whereas the organic only samples showed no difference when compared to an unirradiated monoamide solution. Interestingly, although the product distribution is affected by contact with the acidic aqueous phase, the overall rate of monoamide degradation is not.

**Radical cation reactions with DEH*i*BA**

The irradiation of non-acid contacted dodecane results in degradation of the diluent through molecular ionization ($e^-_{solv}$, $C_{12}H_{26}^{+\bullet}$) and C-H/C-C bond breakage ($C_xH_y^\bullet$, $H^\bullet$, $H_2$). Under aerated conditions it would be expected that the carbon-centered radicals ($C_xH_y^\bullet$), the hydrogen atoms ($H^\bullet$) and the solvated electrons ($e^-_{solv}$) would react with dissolved oxygen to form a suite of less-reactive peroxyl ($C_xH_yO_2^\bullet$) and superoxide ($HO_2^\bullet/O_2^{-\bullet}$) radicals. These conditions isolate the diluent radical cation ($C_{12}H_{26}^{+\bullet}$) as the major species that could react with DEH*i*BA.

Therefore, in this study, we also elucidated the kinetics of this radical cation reaction with DEH*i*BA in dodecane. These fast, pulsed, electron radiolysis experiments were performed as detailed previously,[17] using 0.50 M $CH_2Cl_2$/aerated dodecane to isolate the radical cation with its absorbance directly monitored at 800 nm. Typical kinetic data for the decay of this species are seen in Figure 7. Upon addition of DEH*i*BA the decay becomes faster. From the analysis of the shown decay curves the plot shown in Figure 7 (inset) is derived. The slope of this plot gives the second-order rate constant for the reaction of $C_{12}H_{26}^{+\bullet}$ with DEH*i*BA as $k = (1.52 \pm 0.11) \times 10^{10}$ $M^{-1}$ $s^{-1}$:

$$C_{12}H_{26}^{+\bullet} + \text{DEH}i\text{BA} \rightarrow C_{12}H_{26} + [\text{DEH}i\text{BA}]^{+\bullet} \quad (1)$$

This effectively diffusion-controlled rate constant suggests that this reaction would be an important process in the overall organic phase degradation of this ligand, and supports the hypothesis that it may account for the appearance of m/z 310.2 when it occurs in the organic-only solution.

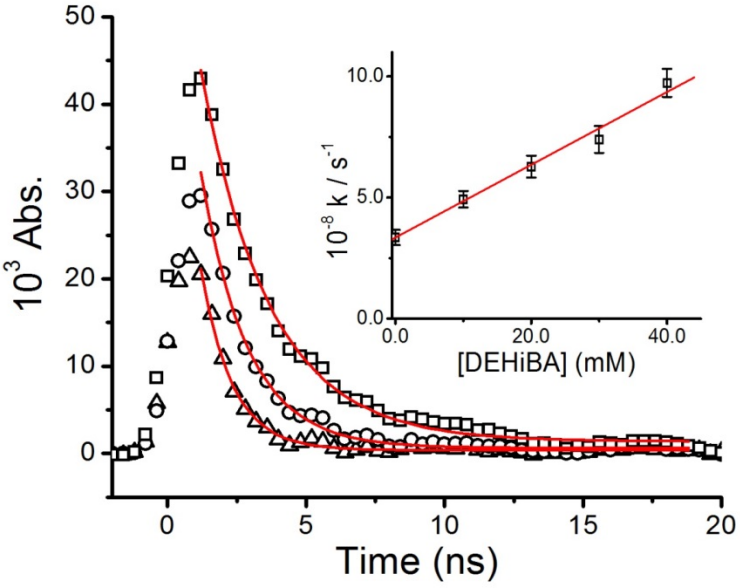


**Figure 7**. Transient absorption decays measured at 800 nm for dodecane radical cation reaction with 10 (□), 20 (O) and 40 (Δ) mM DEH*i*BA at 22°C. Solid lines are fitted double-exponential decays. Inset: Rate constant determination using fast exponent fit values from kinetic traces. Slope of this line corresponds to second-order rate constant of $k = (1.52 \pm 0.11) \times 10^{10}$ $M^{-1}$ $s^{-1}$, $R^2 = 0.99$.

**Degradation product analysis**

Although the overall rate of decrease in concentration was fairly consistent under different conditions of aqueous phases and air sparging, the yields of DEHA and EH*i*BA varied with conditions. In the deaerated organic solution, EH*i*BA yields were low, with DEHA being the favored product. This is shown in Fig. 8. The very reducing conditions of the deaerated dodecane solution favored rupture of the carbonyl C–N bond (Scheme 2). The attack at this bond must be

initiated by direct effect products of dodecane; either solvated electrons, their corresponding radical cations, the •H atom, or a combination of these species. These are also the conditions under which the higher molecular weight C-radical addition products were found. When organic-only samples were air sparged, the yield of DEHA dropped, probably due to oxygen scavenging of either solvated electrons or •H atoms that were previously responsible for the carbonyl C–N bond rupture.

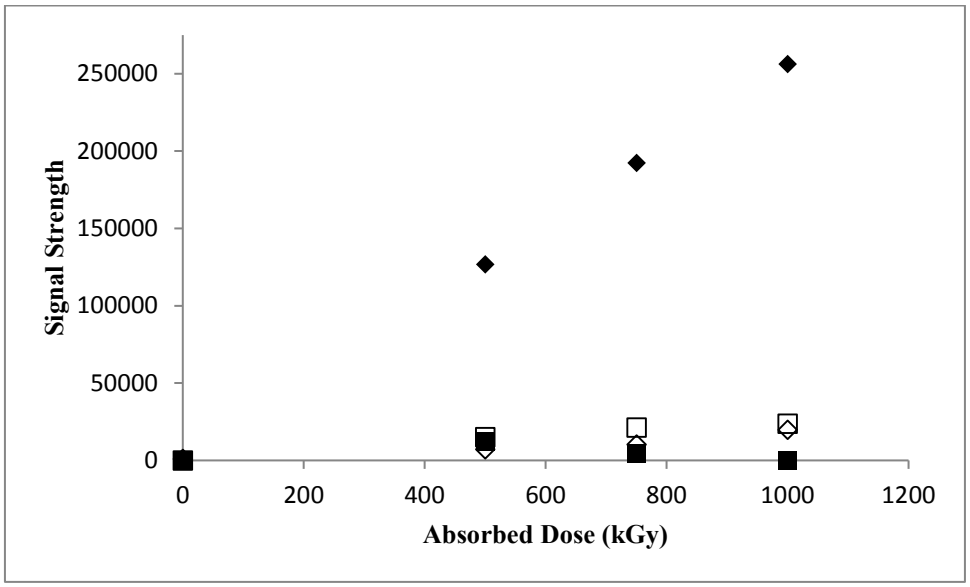


**Figure 8**. Yields of DEHA (m/z 242; diamonds) and EH*i*BA (m/z 200; squares) in irradiated 1 M DEH*i*BA/dodecane for deaerated (closed symbols) and air-sparged solution (open symbols). A relative standard deviation of ± 11 % may be calculated based on quintuplicate analyses.

For the samples irradiated in the presence of 0.1 M $HNO_3$, shown in Fig. 9, the DEHA yield was lower, although it was still produced in highest yield in the deaerated solution. It was essentially suppressed when aerated. Since the dilute $HNO_3$ is expected to quantitatively scavenge radiolytically-produced electrons, the DEHA production is attributed to •H atom reactions, and aeration further suppresses the yield through oxygen scavenging of that radical. Interestingly, aeration may have somewhat increased the yield of EH*i*BA in both the neat organic

and 0.1 M $HNO_3$-contacted solutions, perhaps indicating a role for peroxyl radical formation by oxygen addition to a C-centered radical for this product.

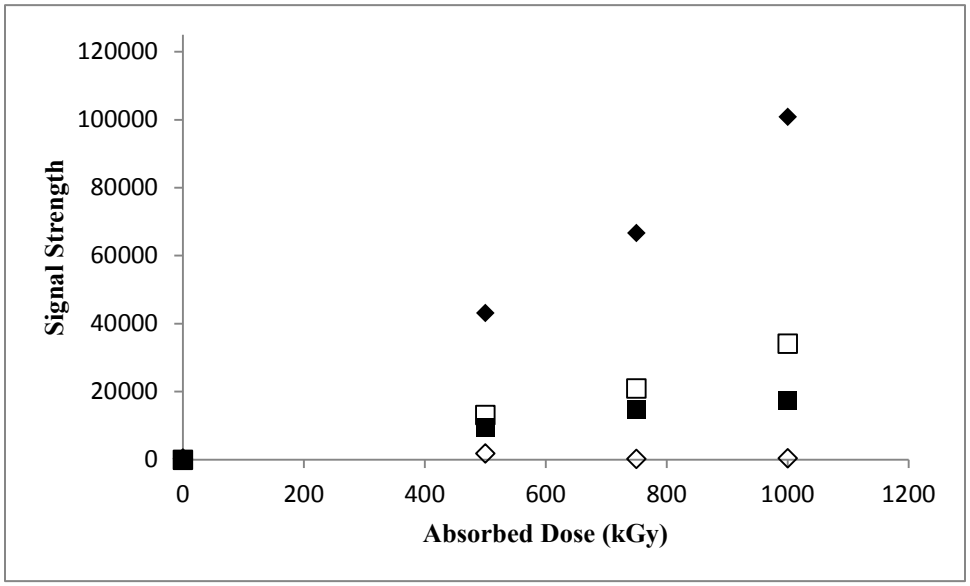


**Figure 9**. Yields of DEHA (m/z 242; diamonds) and EH*i*BA (m/z 200; squares) in the organic phase of 1 M DEH*i*BA/dodecane irradiated under process strip conditions of contact with 0.1 M $HNO_3$, for deaerated (closed symbols) and air-sparged solution (open symbols). A relative standard deviation of ± 11 % may be calculated based on quintuplicate analyses.

The irradiations in contact with 4 M $HNO_3$, shown in Fig. 10, are the most oxidizing conditions studied, providing high yields of both $^{\bullet}OH$ and $^{\bullet}NO_3$ radicals. The product yields are now reversed. Production of EH*i*BA was favored (Scheme 1), and its yield was again highest in the air-sparged solution. Thus it is concluded that DEHA is a reduction product, and that EH*i*BA is an oxidation product of DEH*i*BA radiolysis.

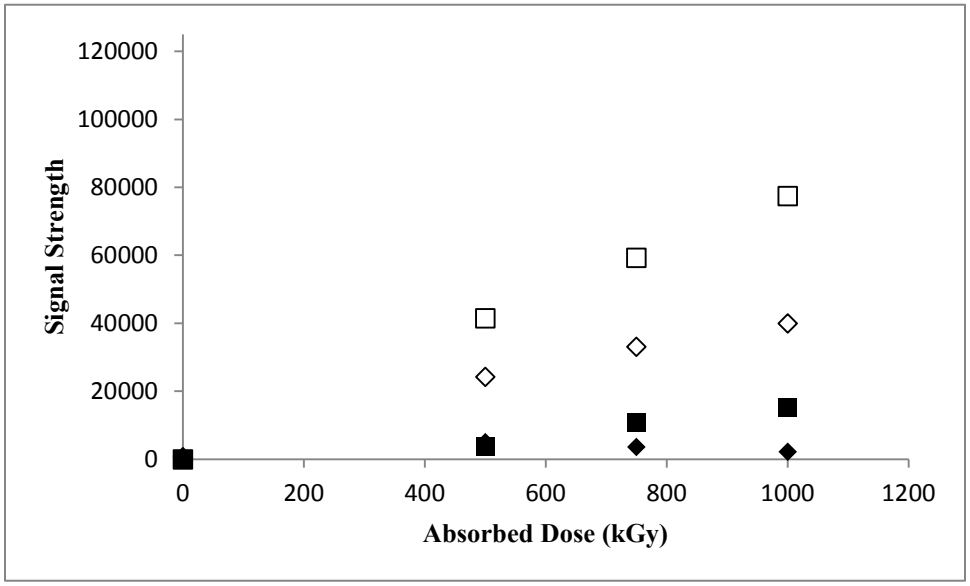


**Figure 10**. Yields of DEHA (m/z 242; diamonds) and EH*i*BA (m/z 200; squares) in the organic phase of 1 M DEH*i*BA/dodecane irradiated under process extraction conditions of contact with 4.0 M $HNO_3$, for deaerated (closed symbols) and air-sparged solution (open symbols). A relative standard deviation of ± 11 % may be calculated based on quintuplicate analyses.

As shown in Fig. 2, the dose constants for DEH*i*BA degradation were invariant across all irradiation conditions, yet as shown in Figs. 8–10 the yields of the major products DEHA and EH*i*BA were very different. Absolute product concentrations cannot be detemined, and signal strengths may vary between mass spectrometric analytical campaigns and thus mass balance analysis for the products cannot be performed. However, from a qualitative point of view it seems clear that mass balance is not achieved based on DEHA and EH*i*BA alone, and that products with lower molecular weights than detectable here must occur, especially under oxidizing conditions. Oxygen addition to C-centered radicals is known to degrade organic compounds to carboxylic acids, ketones and aldehydes via decomposition of their peroxyl radical

intermediates and may account for low molecular weight radiolysis product species, especially in air sparged solution. Further, for samples irradiated in the presence of an aqueous phase, substantial solubility of products in that phase may also occur and would be unaccounted for by organic phase analysis.

**Aqueous phase analysis**

To aide in the understanding of the impact of acid during irradiation on monoamide degradation, the aqueous phase was next analyzed to determine if degradation products could be observed. The nature of the species identified in the aqueous phase by ESI-MS appears to depend on nitric acid concentration. Fig. 11 shows the spectra of the 0.1 M $HNO_3$ irradiated DEH*i*BA aqueous phase and Fig. 12 shows the 4 M $HNO_3$ sample. There are more species present in the 4 M $HNO_3$ sample than in the 0.1 M $HNO_3$ sample.

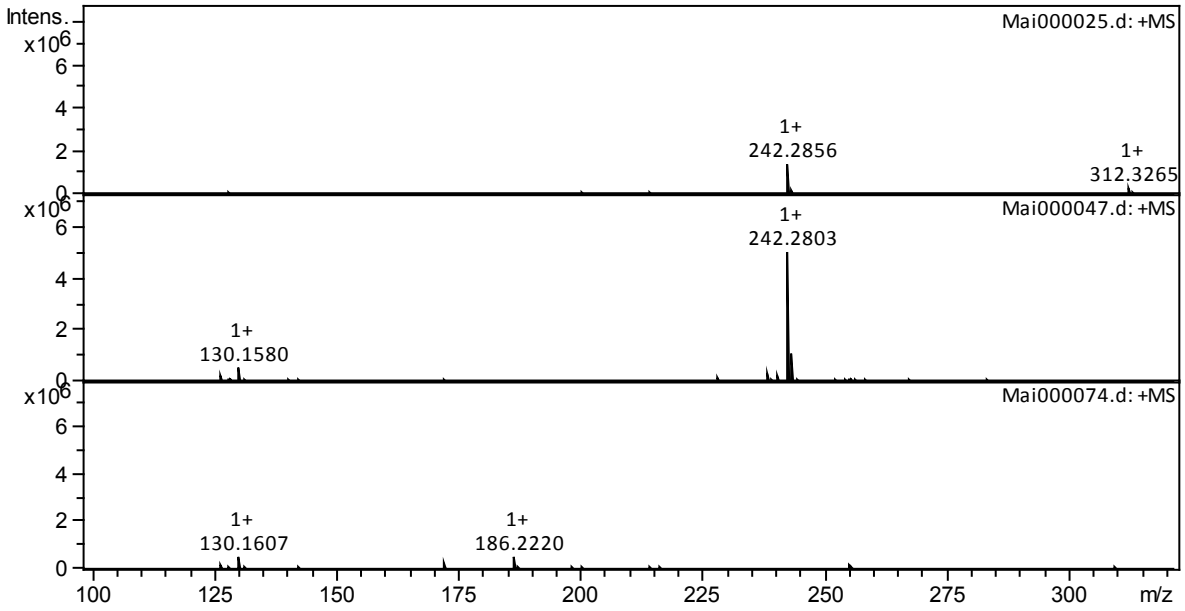


**Figure 11**. ESI-MS spectra of aqueous phase samples of DEH*i*BA at 0 kGy (top), 500 kGy (middle), 1000 kGy (bottom) contacted with 0.1 M $HNO_3$. All spectra were recorded in positive ionization mode, trap drive 50, skimmer voltage 30 V, air sparged.

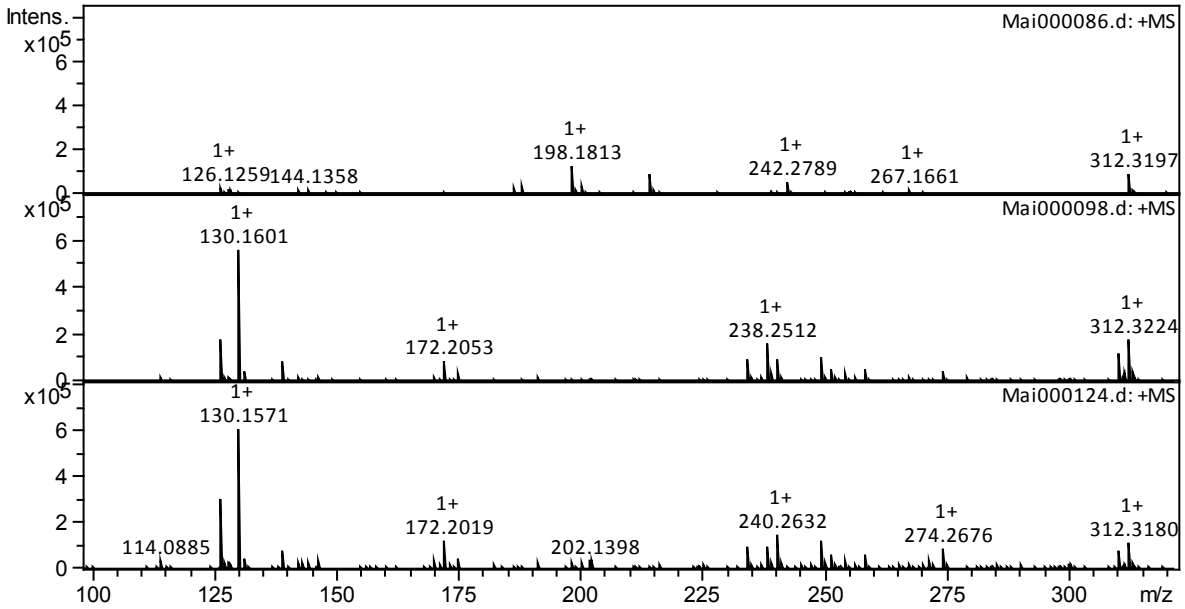


**Figure 12. ESI-MS s**pectra of aqueous phase samples of DEH*i*BA at 0 kGy (top), 500 kGy (middle), 1000 kGy (bottom) contacted with 4 M $HNO_3$. All spectra were recorded in positive ionization mode, trap drive 50, skimmer voltage 30 V, air sparged.

The products DEHA (m/z 242.2) and EH*i*BA (m/z 200.2) were found in both the 0.1 M and 4.0 M $HNO_3$ aqueous phases of the irradiated samples, with maximum signal strength in the samples irradiated between 500–750 kGy. This is shown for samples irradiated in contact with 4 M $HNO_3$ in Fig. 13. A new product was detected at m/z 130.3. It has been identified as 2-ethylhexyl-amine, indicating loss of both a butyl and one ethylhexyl group, likely produced by continued radiolysis of either DEHA or EH*i*BA. The concentrations of these products decreased at higher absorbed doses, suggesting that these species are susceptible to continued radiolysis in the aqueous phase, and as their signals decreased, the high-intensity signal at m/z 130.3 (2-ethylhexylamine) grew in. This signal continued to increase to a maximum at the highest absorbed dose of 1000 kGy.

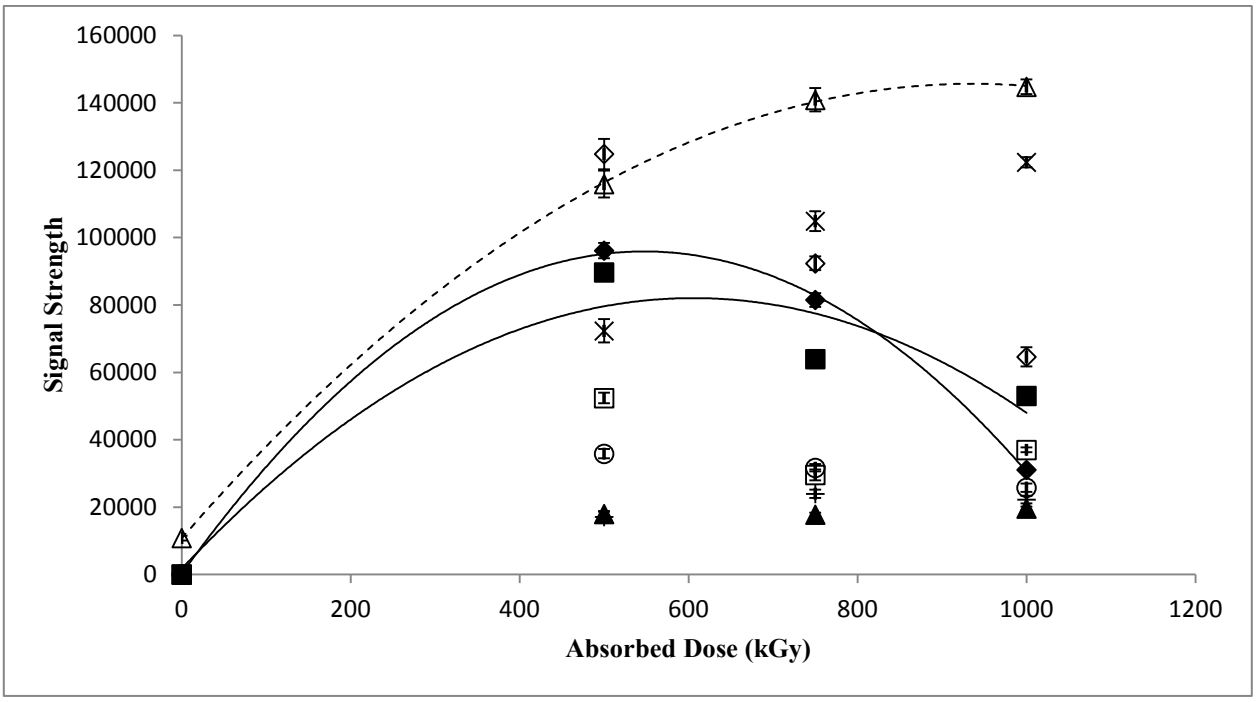


**Figure 13**. Yield of products in the aqueous phase found for initially 1 M DEH*i*BA/dodecane irradiated in contact with aerated 4 M $HNO_3$: DEHA (m/z 242; closed diamonds); EH*i*BA (m/z 200; closed squares); 2-ethylhexylamine (m/z 130, triangles); diethylhexylhydroxylamine (m/z 258, circles); (m/z 310, open diamonds); (m/z 326, open squares); (m/z 126, x); and (m/z 142, +). The parent DEH*i*BA also occurred at low signal strength (closed triangles). Polynomial fits given for DEHA, EH*i*BA and mz 310 are meant solely to guide the eye. A relative standard deviation of ± 11 % may be calculated based on quintuplicate analyses.

An unidentified ion increases in abundance with increased dose in the 4.0 M $HNO_3$, air-sparged samples at m/z 142.2, and another unidentified ion was radiolytically-produced at m/z 126.2 (possibly C8H15NO). The continued degradation of the DEHA and EH*i*BA to lower molecular weight, highly oxidized species was favored under the oxidizing conditions of aeration in the presence of strong $HNO_3$. Small amounts of the parent monoamide were also identified in the aqueous phase. All ions detected in the aqueous phase are shown in Table 3.

**Table 3**. Compounds observed in the aqueous phase as a function of experimental conditions. L stands for DEH*i*BA. N.S. stands for Non Sparged samples and S for sparged samples

| m/z | Formula | 0.1 M $HNO_3$ | | 4 M $HNO_3$ | |
|---|---|---|---|---|---|
| | | N. S. | S. | N. S. | S. |
| 126.2 | $[C_8H_{15}N]H^+$ | X | X | X | X |
| 130.3 | $[C_8H_{19}N]H^+$ | X | X | X | X |
| 139.1 | | | | X | |
| 140.2 | | | X | | |
| 142.2 | | X | X | | X |
| 144.1 | | | X | | |
| 170.1 | | | | | X |
| 172.2 | | X | | X | |
| 186.2 | | X | | | |
| 198.2 | $[C_{12}H_{22}NO]H^+$ | X | X | | X |
| 200.2 | $[C_{12}H_{24}NO]H^+$ | X | | X | X |
| 202.2 | | | | X | X |
| 214.2 | | X | X | X | |
| 234.1 | | | | | X |
| 238.2 | $[C_{16}H_{31}N]H^+$ | | | X | X |
| 240.2 | $[C_{16}H_{33}N]H^+$ | X | | X | X |
| 242.2 | $[C_{16}H_{35}N]\ H^+$ | X | X | | |
| 254.2 | $[C_{16}H_{31}NO]H^+$ | | | | X |
| 255.3 | | X | | | |
| 256.0 | $[C_{16}H_{33}NO]H^+$ | | X | | |
| 258.2 | $[C_{16}H_{35}NO]H^+$ | | | | X |
| 274.2 | | | | | X |
| 310.2 | $[C_{20}H_{39}NO]H^+$ | | X | X | X |
| **312.2** | **LH+** | | X | X | X |
| 326.0 | $[C_{20}H_{39}NOO]H^+$ | | | X | X |
| 328.0 | $[C_{20}H_{40}NOOH]H^+$ | | | X | |
| **334.2** | **$LNa^+$** | | | | |
| 340.2 | $[C_{20}H_{37}NO_3]H^+$ | | | X | X |

**Effects of irradiation on uranium solvent extraction**

The $D_U$ for the extraction of non-irradiated DEH*i*BA was consistent with expectations based on literature results.[2,4] It can be seen in Fig. 14 that within the ± 8% uncertainty, there was no change in uranium extraction efficiency with absorbed dose to the maximum of 1000 kGy under any irradiation condition. This is consistent with the high stability of DEH*i*BA under all conditions, the generation of decomposition products such as EH*i*BA that are likely also

extractants, and also the excess initial concentration of the ligand in comparison with the tracer metal concentration (0.01 mM). It can also be seen in Fig. 14 that the stripping $D_U$ appears to gradually decrease with absorbed dose. This may be a result of the presence of DEH*i*BA radiolysis products in the aqueous strip solution, and the corresponding stripping of uranium by these species. Although the decreases in $D_U$ are not large, decreased stripping distribution ratios can only be considered to be advantageous to a process separation.

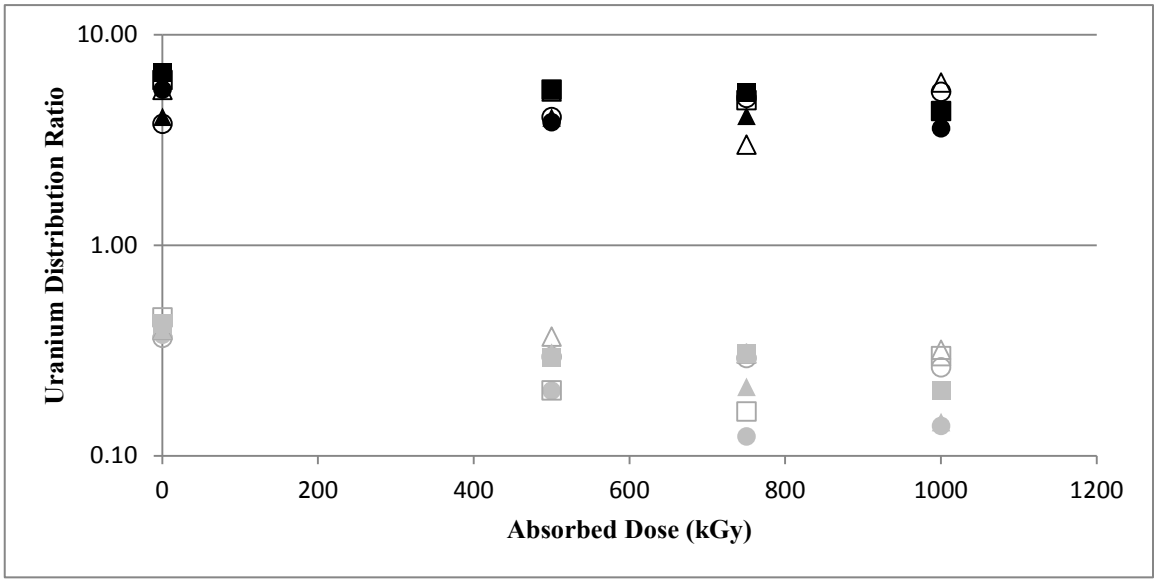


**Figure 14**. Uranium solvent extraction ($D_U$) from 6.5 M $HNO_3$, (black symbols) and stripping, (grey symbols) using irradiated, initially 1 M DEH*i*BA in dodecane. Irradiated organic phase only (open circles); sparged organic phase (filled circles); contact with 0.1 M $HNO_3$ (open triangles); sparged contact with 0.1 M $HNO_3$ (closed triangles); contact with 4 M $HNO_3$ (open squares); and sparged contact with 4 M $HNO_3$ (closed squares). Mean error bars of ± 8 % omitted for clarity.

## CONCLUSIONS

The radiolytic degradation rate of DEH*i*BA is similar to that of TBP and malonamides, and slow compared to the DGAs, and is unaffected by contact with an aqueous phase or aeration. However, product distributions vary with irradiation conditions. Based on these results, DEH*i*BA

apparently undergoes degradation via two pathways: an acid promoted pathway, Scheme 1, and an acid independent pathway, Scheme 2. It is clear that the monoamide degrades when irradiated in the presence of an aqueous phase to form a series of lower molecular weight species generated from the cleavage of the C-N amide bond or C-N amine bond. As this is the active site during synthesis, it is not surprising that this is the weak point in the ligand structure. The main degradation products appear to be DEHA and EH*i*BA. These species, and the smaller fragments produced by their radioysis have increased solubility in the aqueous phase. Another product common to all irradiation conditions was the species at m/z 310.2, which is identified as an unsaturated derivative of DEH*i*BA, resulting from the loss of two H-atoms.

In contrast, when an aqueous phase is not present, higher molecular weight products are generated via carbon radical addition reactions under the more reducing conditions. These products have maximum abundance at 750 kGy, and then decrease with increasing absorbed dose. Their significance to a biphasic solvent extraction process is probably inconsequential.

Solvent extraction results show that DEH*i*BA radiolytic degradation had little effect on uranium distribution ratios even at absorbed doses as high as 1 MGy. The build-up of degradation products in the aqueous phase apparently decreased stripping distribution ratios, which is not adverse to a process application. Thus, these findings for DEH*i*BA are in agreement with previous work that claimed good radiation stability and generation of inoffensive radiolysis products for the monoamides. This, in addition to their CHON nature suggests that they will be good candidates for the development of advanced fuel cycles. Interesting future work would include a comparison study on the *n*-alkane monoamide DEHBA.

## REFERENCES

1. Gasparini, G. M. and Grossi, G., Long-chain disubstituted aliphatic amides as extracting agents in industrial applications of solvent-extraction, *Solvent Extraction and Ion Exchange*, **1986**, 4, 1233–1271.
2. Siddall, T. H., Effects of structure of N,N-disubstituted amides on their extraction of actinide and zirconium nitrates and of nitric acid, *Journal of Physical Chemistry*, **1960**, 64, 1863–1866.
3. Pathak, P. N., Kumbhare, L. B. and Manchanda, V. K., Structural effects in N,N-dialkyl amides on their extraction behavior toward uranium and thorium, *Solvent Extraction and Ion Exchange*, **2001**, 19, 105–126.
4. Prabhu, D. R., Mahajan, G. R. and Nair, G. M., Di(2-ethyl hexyl)butyramide and di(2-ethyl hexyl)isobutyramide as extractants for uranium(VI) and plutonium(IV), *Journal of Radioanalytical and Nuclear Chemistry*, **1997**, 224, 113–117.
5. Mowafy, E. A., The effect of previous gamma-irradiation on the extraction of U(VI), Th(IV), Zr(IV), Eu(III) and Am(III) by various amides, *Journal of Radioanalytical and Nuclear Chemistry*, **2004**, 260, 179–187.
6. Ruikar, P. B., Nagar, M. S. and Subramanian, M. S., Extraction behavior of uranium, plutonium and some fission-products with gamma-irradiated n,n'-dialkylamides, *Journal of Radioanalytical and Nuclear Chemistry-Articles*, **1992**, 159, 167–173.
7. Ruikar, P. B., Nagar, M. S. and Subramanian, M. S., Extraction of uranium, plutonium and some fission-products with gamma-irradiated unsymmetrical and branched-chain dialkylamides, *Journal of Radioanalytical and Nuclear Chemistry-Letters*, **1993**, 176, 103–111.
8. Parikh, K. J., Pathak, P. N., Misra, S. K., Tripathi, S. C., Dakshinamoorthy, A. and Manchanda, V. K., Radiolytic Degradation Studies on N,N-dihexyloctanamide (DHOA) under PUREX Process Conditions, *Solvent Extraction and Ion Exchange*, **2009**, 27, 244–257.
9. Pathak, P.N.; Prabhu, D.R.; Kanekar, A.S.; Manchanda, V.K. Evaluation of *N,N*-dialkylamides as promising process extractants. IOP Conf. Series: Materials and Science Engineering 9, 2010, 012082.
10. Ruikar, P. B., Nagar, M. S., Subramanian, M. S., Gupta, K. K., Varadarajan, N. and Singh, R. K., Extraction behavior of uranium(VI), plutonium(IV) and some fission-products with gamma-pre-irradiated n-dodecane solutions of N,N'-dihexyl substituted amides, *Journal of Radioanalytical and Nuclear Chemistry-Articles*, **1995**, 196, 171–178.
11. Pathak, P. N., Prabhu, D. R., Ruikar, P. B. and Manchanda, V. K., Evaluation of Di(2-éthylhexyl)isobutyramide (D2EHiBA) as a process extractant for the recovery of $^{233}U$ from irradiated Th, *Solvent Extraction and Ion Exchange*, **2002**, 20, 293–311.
12. Manchanda, V. K. and Pathak, P. N., Amides and diamides as promising extractants in the back end of the nuclear fuel cycle: An overview, *Separation and Purification Technology*, **2004**, 35, 85–103.
13. Musikas, C., Solvent-extraction for the chemical separations of the 5f elements, *Inorganica Chimica Acta*, **1987**, 140, 197–206.
14. Musikas, C., Potentiality of nonorganophosphorus extractants in chemical separations of actinides, *Separation Science and Technology*, **1988**, 23, 1211–1226.

15. Mincher, B.J., Modolo, G., Mezyk, S.P. The effects of radiation chemistry on solvent extraction: 1. Conditions in Acidic Solution and a Review of TBP Radiolysis. *Solvent Extraction and Ion Exchange,* **2009**, 27, 1–25.
16 Fricke, H., Hart, E. The chemical action of roentgen rays on dilute ferrosulphate solutions as a measure of dose. *Am. J. Roent. Radium Ther. Nucl. Med*. **1927**, 18, 430–432.
17. Zarzana, C. A., Groenewold, G. S., Mincher, B. J., Mezyk, S. P., Wilden, A., Schmidt, H., Modolo, G., Wishart, J. F. and Cook, A. R., A Comparison of the gamma-Radiolysis of TODGA and T(EH)DGA Using UHPLC-ESI-MS Analysis, *Solvent Extraction and Ion Exchange*, **2015**, 33, 431–447.
18. Galan, H., Zarzana, C. A., Wilden, A., Nunez, A., Schmidt, H., Egberink, R. J. M., Leoncini, A., Cobos, J., Verboom, W., Modolo, G., Groenewold, G. S. and Mincher, B. J., Gamma-radiolytic stability of new methylated TODGA derivatives for minor actinide recycling, *Dalton Transactions*, **2015**, 44, 18049–18056.
19. Roscioli-Johnson, K.M.; Zarzana, C.A.; Groenewold, G.S.; Mincher, B.J.; Wilden, W.; Schmidt, H.; Modolo, G.; Santiago-Schübel, B. A study of the γ-radiolysis on N,N-didodecyl-N'N'-dioctyldiglycolamide using UHPLC-ESI-MS analysis. *Solvent Extraction and ion Exchange*, **2016**, 34, 439–453.
20. Berthon, L., Morel, J. M., Zorz, N., Nicol, C., Virelizier, H. and Madic, C., Diamex process for minor actinide partitioning: Hydrolytic and radiolytic degradations of malonamide extractants. *Separation Science and Technology*, **2001**, 36, 709–728.
21. Adamov, V.M., Andreev, V.I., Belyaev, B.N., Markov, G.S., Polyakov, M.S., Ritari, A.E., Shil'nikov, A. Yu. Radiolysis of an extraction system based on solutions of tri-n-butylphosphate in hydrocarbon diluents. *Sov Radiochem* **1988**, 29, 775–781.
22. Condamines, N. and Musikas, C., The extraction by N,N- dialkylamides.I. $HNO_3$ and other inorganic acids. *Solvent Extraction and Ion Exchange*, **1988**, 6, 1007–1034.
23. Dejugnat, C., Berthon, L., Dubois, V., Meridiano, Y., Dourdain, S., Guillaumont, D., Pellet-Rostaing, S. and Zemb, T., Liquid-liquid extraction of acids and water by a malonamide: I-anion specific effects on the polar core microstructure of the aggregated malonamide. *Solvent Extraction and Ion Exchange*, **2014**, 32, 601–619.